applied sciences

MDPI

Article

Nonlinear Dynamics of a Piezoelectric Bistable Energy Harvester Using the Finite Element Method

Virgilio J. Caetano [1] and Marcelo A. Savi [2,*]

[1] Department of Aeronautical Engineering, Escola de Engenharia de São Carlos, Universidade de São Paulo, São Carlos 13566-590, SP, Brazil; vj.caetano@usp.br
[2] COPPE, Mechanical Engineering, Center for Nonlinear Mechanics, Universidade Federal do Rio de Janeiro, Rio de Janeiro 21941-617, RJ, Brazil
* Correspondence: savi@mecanica.coppe.ufrj.br

Abstract: The conversion of ambient mechanical vibrational energy into electrical energy through piezoelectric devices has received an increasing attention in recent years. The main challenges are to develop efficient devices that operate over a wide frequency range, adapting to diverse environmental energy sources. This work presents a framework for the analysis of a nonlinear vibration-based energy harvesting devices combining the nonlinear finite element method with a reduced-order model, which provides a broader dynamical investigation. On this basis, a flexible tool is developed, allowing the multimodal analysis of nonlinear systems. A bistable piezoelectric energy harvesting device is investigated considering the influence of multimodal and nonlinear effects on the system performance. Bistability is due to magnetic interactions among magnets and the beam tip, modeled by cubic nonlinearities. Numerical simulations show the influence of vibration sources on the dynamics and performance of the device. Nonlinear effects furnish rich dynamics, presenting periodic and chaotic responses. All these effects can be combined to enhance energy harvesting capacity.

Keywords: energy harvesting; finite element method; nonlinear dynamics; smart materials; piezoelectricity

Academic Editors: Matteo Strozzi and Giovanni Iarriccio

Received: 28 January 2025
Revised: 10 February 2025
Accepted: 11 February 2025
Published: 14 February 2025

Citation: Caetano, V.J.; Savi, M.A. Nonlinear Dynamics of a Piezoelectric Bistable Energy Harvester Using the Finite Element Method. *Appl. Sci.* **2025**, *15*, 1990. https://doi.org/10.3390/app15041990

1. Introduction

Energy harvesting from ambient sources has gathered considerable focus due to its structural simplicity and high conversion capacity. The investigation of energy conversion from mechanical vibrations into electrical energy has become an important field of research in recent decades due to its great potential to replace/recharge batteries in wireless sensors and low-power-consuming electronic devices. The most common devices are based on a cantilever beam with piezoelectric transduction, known as the piezoelectric beams [1–4]. The literature presents a wide variety of works based on piezoelectric cantilever beam models analyzed through linear devices [5–9]. These linear devices are suitable for stationary excitation with bandwidth close to the natural frequency, under resonant conditions, becoming less efficient when the ambient vibration energy is distributed over a wider frequency spectrum. This fact stimulated the investigation of different devices that amplify the limited bandwidth of linear systems [10,11].

An alternative to overcome the narrow operational bandwidth of linear devices is the consideration of multi-degrees-of-freedom systems, including harvester arrays [12,13] and multimodal structures [14–18]. These devices have different response peaks and can be designed to obtain close resonant frequencies, increasing the operating range of the system.

Different design configurations can be imagined in order to reach this goal. Caetano and Savi [19] proposed a pizza-shaped irregular structure while Caetano and Savi [20] proposed a star-shaped structure exploiting the same idea. In addition, different configurations can be employed to aggregate multidirectionality to the device. In this regard, Caetano and Savi [20] showed that the incorporation of pendulum masses can propitiate the multi-directional aspects necessary to deal with direction uncertainty on the energy sources. Dual-beam design combining multiple degrees of freedom and compactness is explored by Costa and Savi [21,22].

Nonlinearities are another attempt to increase the performance of energy harvesting devices. In this regard, multistable energy harvesting devices attracted attention due to their unique characteristics, creating different equilibrium configurations that can be explored to increase energy harvesting capacity [21–23]. Among various piezoelectric energy-harvesting structures, permanent magnets are often used in conjunction with these structures by exploiting magnetic coupling to design monostable [24,25], bistable [26,27] and multistable [28–31] nonlinear energy harvesters. Tang et al. [32] employed magnets in vibration energy harvesters to investigate both monostable and bistable configurations at various excitation levels to improve the performance of conventional linear energy harvesters. The primary advantage of a bistable system over a monostable system is that inter-well motion can cause a significant deformation, resulting in higher output power. However, these configurations are associated with energetic barriers that need to be overcome to reach interesting behaviors for energy harvesting [33,34]. Consequently, the energy source needs to have an energy level high enough for a good harvesting performance since low energy levels impose situations where the system cannot overcome energetic barriers, presenting a poor performance [34]. Multistable energy harvesters with magnetic coupling have been investigated to facilitate overcoming these barriers when compared with bistable configurations, generating high energy output over a broader range of frequencies [28,35]. The main drawback is the added complexity in system dynamics and energy conversion. Nonlinear energy harvesting devices are investigated for different types of ambient excitation, such as harmonics [36,37] and random [38,39], showing a considerable increase in energy generation.

The nonlinear magnetic force is a critical factor influencing the energy scavenging efficiency and the dynamic behavior of vibration-based systems. The magnetic force can primarily be obtained from experimental measurement, numerical simulation, and analytical calculations [29]. While experimental measurements limit the description of nonlinear magnetic force when system parameters change, numerical simulations can accurately estimate magnetic force with parametric variation, but it requires considerable computational cost. Although nonlinear magnetic forces in energy harvesting systems are calculated employing magnetic dipole method, equivalent magnetizing current model, or magnetic charge model, some researchers express magnetic forces by fitting odd-order polynomials for some specific situations. In particular, theoretical analysis of a Duffing-type system is a relatively common modeling alternative to investigating energy harvesters with magnetic coupling [34,36,38,40]. This strategy accurately represents nonlinear dynamical systems, considerably reducing the modeling complexity.

The literature presents analytical and numerical solutions of piezoelectric energy harvesting devices based on simple structures. However, the modeling of complex structures is related to difficulties to accurately describe their behaviors. In this regard, the finite element method (FEM) is an alternative for the analysis of these energy harvesting systems. Various attempts have been used to model piezoelectric energy harvesters through FEM [41–44]. Zhu et al. [41] presented a coupled piezoelectric-circuit model to analyze the power output of the system. Abdelkefi et al. [42] compared analytical and finite element

(FE) models with experimental results presenting good agreements. Concerning nonlinear devices, Upadrashta and Yang [43] proposed a technique to study devices with magnetic interaction by using a nonlinear spring element to model magnetic forces. Recently, the authors investigated a three degrees-of-freedom system to harvest electrical energy from wideband, low-frequency, and low-amplitude ambient vibrations. Caetano and Savi [19,20] employed the FEM to investigate novel energy harvesting designs as pizza-shaped and star-shaped structures.

Although many efforts have been made, the design of efficient energy harvesting devices capable of adapting to different ambient vibration sources remains a challenging task. This work presents a framework for the analysis of a nonlinear vibration-based energy harvesting devices combining the nonlinear finite element method with a reduced-order model, allowing a broader dynamical investigation. The device harvester is a bistable piezoelectric beam where the nonlinear behavior is due to magnetic interactions exerted by magnets in the beam tip. Ambient vibration sources are represented by harmonic base excitation. The use of the finite element method defines a flexible representation that allows multimodal analysis over a wide frequency range. Since the nonlinear dynamics perspective is essential for the design of the energy harvester, this framework allows a broader representation of the system, exploiting the better possibilities for proper operational conditions. Numerical simulations of the finite element model are developed using ANSYS 17 software and results show a qualitative agreement with reduced-order model described by ordinary differential equations. The system presents rich dynamical responses of the device, including chaos. The framework shows the importance to employ a proper model to describe the system dynamics, which can identify enhanced operational conditions.

2. Piezoelectric Energy Harvester

A vibration-based energy harvester is employed to convert mechanical into electrical energy. Essentially it is a resonator that is designed to match the ambient vibration source, working under resonant conditions. A typical configuration is a cantilever beam with a tip mass that allows the adjustment of resonant frequency. A piezoelectric energy harvesting device is a bimorph cantilever beam schematically presented in Figure 1. The system consists of a three-layer structure, two of piezoelectric material (bimorph) bonded to a substrate beam. The substrate is assumed to be made of aluminum, and the piezoelectric material is a PZT-5A. The electrical circuit is represented by a resistor connected, in series, to PZT's layers to generate power output. In addition, ambient vibration is modeled as harmonic base excitation.

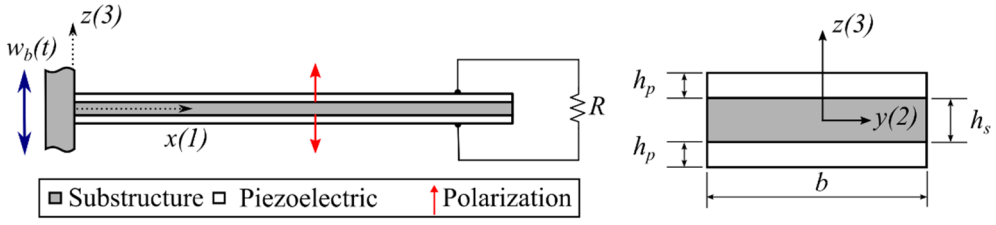

(**a**) (**b**)

Figure 1. Schematic representation of (**a**) linear energy harvester and (**b**) bimorph beam cross section.

Nonlinear effects are usually exploited to enhance the device's energy harvesting capacity, making it more efficient and with wider bandwidth. Among the possible strategies, magnetic interactions are employed conferring multistable behavior to the structure. On this basis, consider that permanent external magnets generate a homogenous magnetic

field that induces a magnetization per unit of length in the beam, producing a force and a magnetic moment. By assuming a beam displacement w, and that $w_L = w(L,t)$ is the displacement of the tip mass, the nonlinearity is due to the dependence of the magnetic force f_{Mz} and the beam tip displacement w_L, as schematically showed in Figure 2, which considers the horizontal distance d_m and the distance between magnets, d_g.

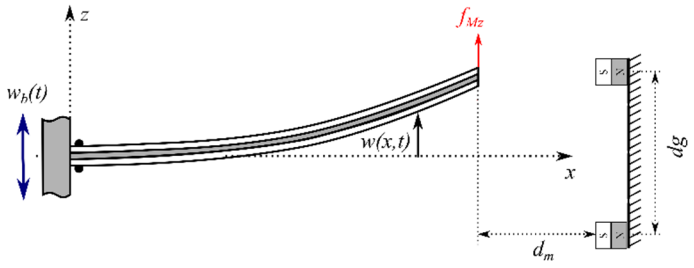

Figure 2. Schematic representation of a nonlinear energy harvesting device comprising a ferromagnetic bimorph beam with magnetic interactions.

A mathematical model is proposed by assuming that the magnets exhibit idealized magnetic behavior with constant properties in time and therefore, magnetic hysteresis and nonlinearities associated with the magnetization and magnetic field relation are neglected. Moreover, magnetic moment and magnetic force in the x-direction are also neglected due to small tip displacement/rotation. Therefore, the magnetic forces are derived following similar procedure presented by Kim and Seok [45], being expressed as follows:

$$f_{Mz} = \sum_{k=1}^{2} \frac{\mu_0}{4\pi} \mathcal{Q}\mathcal{Q}' \left[\frac{w_L - d_h}{\left(d_p^2 + (w_L + g_k)^2\right)^{3/2}} - \frac{w_L - d_h}{\left(d_m^2 + (w_L + g_k)^2\right)^{3/2}} \right] \tag{1}$$

where μ_0 and $\mathcal{Q}$ are the vacuum permeability and total surface charge, respectively; $2l_m$ is the length of each magnet; d_h is half of the distance between magnets (d_g); on this basis, parameters d_p and g_k are defined as: $d_p = d_m + 2l_m$, $g_k = (-1)^k d_h$.

The mathematical model for the nonlinear energy harvesting device is expressed as follows, assuming a Bernoulli-Euler hypothesis for the beam model and an electric circuit represented by a voltage v, with capacitive (C_p) and a resistive load (R),

$$\begin{aligned} YI\frac{\partial^4 w(x,t)}{\partial x^4} + m\frac{\partial^2 w(x,t)}{\partial t^2} - \vartheta\, v(t)\left[\frac{d\delta(x)}{dx} - \frac{d\delta(x-L)}{dx}\right] \\ + c_a\frac{\partial w(x,t)}{\partial t} - f_{Mx}\frac{\partial^2 w}{\partial x^2} = -m\frac{\partial^2 w_b(t)}{\partial t^2} - c_a\frac{\partial w_b(t)}{\partial t} \end{aligned} \tag{2}$$

$$C_p\frac{dv(t)}{dt} + \frac{v(t)}{R} + \vartheta\int_0^L \frac{\partial^3 w(x,t)}{\partial x^2 \partial t}dx = 0 \tag{3}$$

where YI is the equivalent bending stiffness, m is the mass per unit length and ϑ is the piezoelectric coupling. Additionally, c_a is the viscous damping, δ is the Dirac function and $w_b(t)$ is a base excitation. For a bimorph beam configuration, these parameters can be obtained from expressions given in Refs. [2,8] as follows:

$$
\begin{aligned}
YI &= \frac{2b}{3}\left\{Y_s\frac{h_s^3}{8} + \bar{c}_{11}^E\left[\left(h_p+\frac{h_s}{2}\right)^3 - \frac{h_s^3}{8}\right]\right\} \\
\vartheta &= \frac{\bar{e}_{31}b}{2h_p}\left[\left(h_p+\frac{h_s}{2}\right)^2 - \frac{h_s^2}{4}\right] \\
m &= b(\rho_s h_s + 2\rho_p h_p) \\
C_p &= \frac{\bar{\varepsilon}_{33}^S bL}{h_p}
\end{aligned}
\tag{4}
$$

where ρ_s denotes the density, Y_s is the Young's modulus, h_s is the thickness of the substructure; ρ_p, $\bar{c}_{11}^E$ and h_p are related to same properties of piezoelectric material. Moreover, $\bar{\varepsilon}_{33}^S$ is the piezoelectric permittivity coefficient, b is the width and L the length of the composite beam. In addition, the following boundary conditions are adopted,

$$
\begin{gathered}
w(0,t) = 0, \qquad \left.\frac{\partial w}{\partial x}\right|_{x=0} = 0, \qquad \left. YI\frac{\partial^2 w}{\partial x^2}\right|_{x=L} - m_M|_{x=L} = 0, \\
\left. YI\frac{\partial^3 w}{\partial x^3}\right|_{x=L} - f_{Mx}\left.\frac{\partial w}{\partial x}\right|_{x=L} + f_{Mz}|_{x=L} = 0.
\end{gathered}
\tag{5}
$$

The terms with magnetic force in the x-direction (f_{M_x}) in Equations (2) and (5) can be neglected for small beam tip displacement/rotation and, therefore, the nonlinearity is due to the nonlinear dependence of magnetic force f_{Mz} and the beam tip displacement w_L. Geometric and material properties are presented in Table 1.

Table 1. Geometric and material properties of energy device.

Parameters	Substrate	Piezoceramic
Material	Aluminum	PZT-5A
Length (mm)	30	30
Thickness (mm)	0.5	0.5
Mass density (kg/m^3)	2700	7750
Young Modulus (GPa)	70	61
Poisson's Ratio	0.3	0.3
Piezoelectric constants (pC/N)	—	–171
Dielectric constants (nF/m)	—	15.05
Electrical resistance (Ohm)	1×10^6	
Damping ratio	α = 2.16	β = 5

2.1. Discrete Model

The proper discretization of the continuous energy harvesting model employs the relative transverse vibration of the beam, $w(x,t)$, which is approximated by a finite and convergent series of orthogonal functions $\phi_j(x)$, satisfying the boundary conditions. A discrete model can be obtained by applying the Galerkin method, resulting in a system of $r+1$ ordinary differential equations [46] as follows, where r is the number of degrees of freedom employed in the approximation,

$$
\ddot{q}_j(t) + 2\xi_j\omega_j\dot{q}(t) + \omega_j^2 q_j(t) - v(t)\eta_j - \phi_j(L)f_{Mz}(w_L) = f_j(t) \tag{6}
$$

$$
C_p\dot{v}(t) + \frac{1}{R}v(t) + \sum_{j=1}^{r}\eta_j\dot{q}_j(t) = 0 \tag{7}
$$

in which $q_j(t)$ and ξ_j are, respectively, the nodal coordinates and modal damping with $j = 1, 2, \ldots, r$. The eigenfunctions $\phi_j(x)$ are obtained by solving the undamped free

vibration linear problem for fixed-free boundary conditions, under the assumption of a short-circuit connection [8]. The magnetic force f_{Mz} needs to be properly described as a function of the beam displacement at the end, $x = L$, and therefore, $f_{Mz} = f_{Mz}(w_L)$. By considering just the first vibration mode, the magnetic force can be approximated by a cubic expression,

$$f_{Mz} = \mathscr{a} w_L^3 + \mathscr{b} w_L = \mathscr{a}[\phi(L)q(t)]^3 + \mathscr{b}\phi(L)q(t) \tag{8}$$

where the constants $\mathscr{a}$ and $\mathscr{b}$ are determined using Equation (1) through least-squares fitting, employing the parameters shown in Table 2.

Table 2. Properties of magnets.

Parameters	Piezoceramic
Beam-magnet horizontal spacing (mm)	$d_m = 4.7$
Spacing between magnets (mm)	$d_g = 14$
Magnets length (mm)	$l_m = 4$
Magnets width (mm)	$b_m = 4$
Magnetization (A/m)	12×10^5
Vacuum permeability (N/A^2)	1.26×10^{-6}

On this basis, a Duffing-type nondimensional equation of motion is employed to describe a reduced-order model of the energy harvesting device as follows

$$\begin{cases} \dot{u}_1 = u_2 \\ \dot{u}_2 = -2\xi\dfrac{\omega}{\overline{\omega}}u_2 - \psi u_1 - \mu u_1^3 - \chi u_3 + F_j(t) \\ \dot{u}_3 = -\gamma u_3 - k u_2 \end{cases} \tag{9}$$

where

$$\mu = -\mathscr{a}\phi(L)^4\frac{\overline{L}^2}{\overline{\omega}^2}, \qquad \psi = \frac{1}{\overline{\omega}^2}\left[\omega^2 - \mathscr{b}\phi(L)^2\right] \qquad \text{and} \qquad F_j = -\frac{m}{\overline{L}\overline{\omega}^2}\ddot{w}_b\int_0^L \phi_j(x)dx. \tag{10}$$

This Duffing-type equation is characterized by a cubic nonlinearity, which is associated with a double-well potential of the following type,

$$\Psi_p(u_1) = \frac{1}{2}\psi u_1^2 + \frac{1}{4}\mu u_1^4. \tag{11}$$

2.2. Finite Element Model

The formulation of a nonlinear finite element method can be expressed by the following generic equation by considering the displacement $\boldsymbol{u}$, and the mass matrix, $\boldsymbol{M}$, the damping matrix, $\boldsymbol{C}$, and a forcing term, $\boldsymbol{f}$,

$$\boldsymbol{M}\ddot{\boldsymbol{u}}_{n+1} + \boldsymbol{C}\dot{\boldsymbol{u}}_{n+1} + \boldsymbol{f}^i_{n+1}(\boldsymbol{u}_{n+1}) = \boldsymbol{f}_{n+1} \tag{12}$$

where $\boldsymbol{f}^i$ represents a nonlinear stiffness that depends on the displacement. The Newmark method can be employed to solve this equation, with the residual vector $\boldsymbol{r}_{n+1}(\boldsymbol{u}_{n+1})$ being expressed by

$$\boldsymbol{r}_{n+1}(\boldsymbol{u}_{n+1}) = \boldsymbol{f}_{n+1} - \boldsymbol{f}^i_{n+1} - \boldsymbol{M}\ddot{\boldsymbol{u}}_{n+1} - \boldsymbol{C}\dot{\boldsymbol{u}}_{n+1} \tag{13}$$

The Newton-Raphson method is employed in the solution,

$$\boldsymbol{\mathcal{F}}_{n+1}\left(\boldsymbol{u}_{n+1}^{k}\right)+\frac{\partial \boldsymbol{\mathcal{F}}\left(\boldsymbol{u}_{n+1}^{k}\right)}{\partial \boldsymbol{u}_{n+1}}\Delta \boldsymbol{u}_{n+1}^{k}=0 \tag{14}$$

where $\Delta \boldsymbol{u}_{n+1}^{k}$ is an increment of $\boldsymbol{u}_{n+1}$ as described in detain in Ref. [47].

The energy harvesting system is modeled and analyzed using ANSYS Academic Research 17. Figure 3 shows the FE model of the harvester presented in Figure 1. The substrate beam is modeled with 2D structural element PLANE82, which has 8 nodes and 2 DOFs per node, presenting translation motion in x and y directions. The PZT material is modeled using 2D 8 nodes element, PLANE223, having two translational DOFs and one additional DOF of voltage for each node. In addition, a resistor element (CIRC94) is connected to the PZT elements. A dissipation mechanism is introduced assuming damping proportional to system's mass and stiffness (Rayleigh method) defined by parameters α and β, respectively.

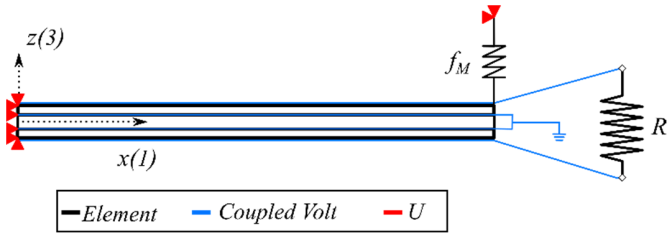

Figure 3. Schematic of FE model of energy harvester with a magnetic force f_M, a resistive load R, boundary displacement conditions U and coupled voltage DOF to emulate the electrodes.

Base excitation is assumed to be harmonic, being imposed by coupling the nodes located at $x = 0$ in a component and applying displacement boundary condition. In addition, the voltage DOF on the upper and lower surfaces are coupled to provide uniform electrical potentials and thus emulate the electrodes of each piezoelectric layer.

The magnetic force exerted at the beam free-end is the essential nonlinear effect involved in the energy harvesting device. This magnetic force is modeled using a nonlinear spring element as proposed by Upadrashta and Yang [43]. ANSYS COMBIN39 element is employed to simulate the magnetic interaction by approximating the nonlinear force with piecewise linear segments. Figure 4 shows the variation in magnetic force (f_{Mz}) with lateral displacement using Equation (1) and the linear fit supplied to COMBIN39 element. This force is applied at a node in the free-end-neutral-axis of the beam. Parameter values used to calculate f_{Mz} are presented in Table 2.

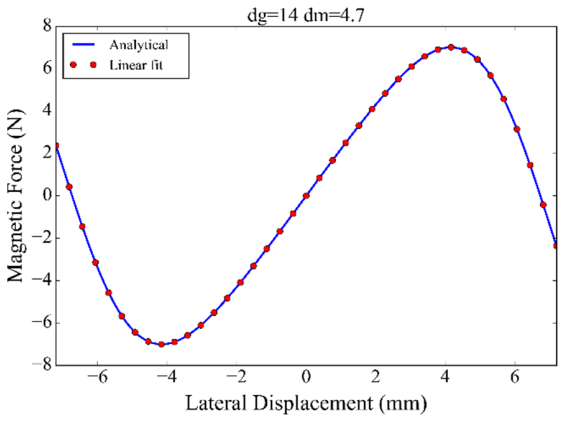

Figure 4. Magnetic force variation with lateral displacement.

3. Numerical Simulations

Numerical simulations are developed to show the system dynamics that define the energy harvesting capacity. The employed models are initially compared with other numerical and experimental tests available in the literature, promoting a model verification. Afterward, the reduced-order model is of concern in order to observe the general characteristics of the system dynamics. The fourth-order Runge–Kutta method is employed considering time steps less than 0.001 s, defined after a convergence analysis. A bifurcation diagram is employed to provide a global comprehension of the system dynamics. This diagram is built by considering a stroboscopic view of the response under slow quasi-static variation in a parameter, using a Poincaré map. Figure 5 presents the bifurcation diagram varying the base displacement (w_0) that represent the external stimulus of Equations (9) and (10), defined as $w_b = w_0 \sin(\Omega\tau)$, with a constant frequency excitation of 70 Hz. There is a noticeable period-1 response followed by bifurcations that reaches a chaotic region and, following this, another period-1 response is reached.

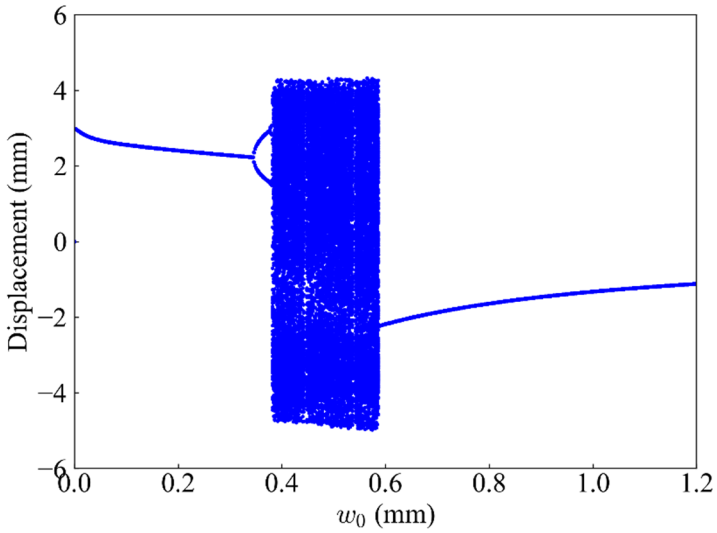

Figure 5. Bifurcation diagram built with the reduced-order model.

Three different types of responses can be identified in terms of energy harvesting capacity, essentially related to motion amplitude and therefore, with the dynamical response. These responses are associated with external stimulus, characterized by forcing amplitude and frequency. The first one is the intra-well behavior, related to low energy stimulus (0.15 mm, 70 Hz), where the system response is characterized by oscillations limited to only one equilibrium point (Figure 6a). The second behavior is a chaotic response (0.4 mm, 70 Hz) presented in Figure 6b: a solution associated with a strange chaotic attractor that visits all equilibrium points. Finally, the third kind of behavior is an inter-well response (1.0 mm, 70 Hz), where both stable equilibrium points are visited.

The reduced-order model scenarios furnish the dynamic perspective of the energy harvester, guiding the more complex investigation of the FE model, which is now in focus. System performance is monitored by considering output voltage. The finite element model uses a structured mesh composed of 6000 elements. Time steps are determined as a function of the excitation frequency (Ω), with at least 40 points per excitation period ($T = 1/\Omega$) ensuring good convergence.

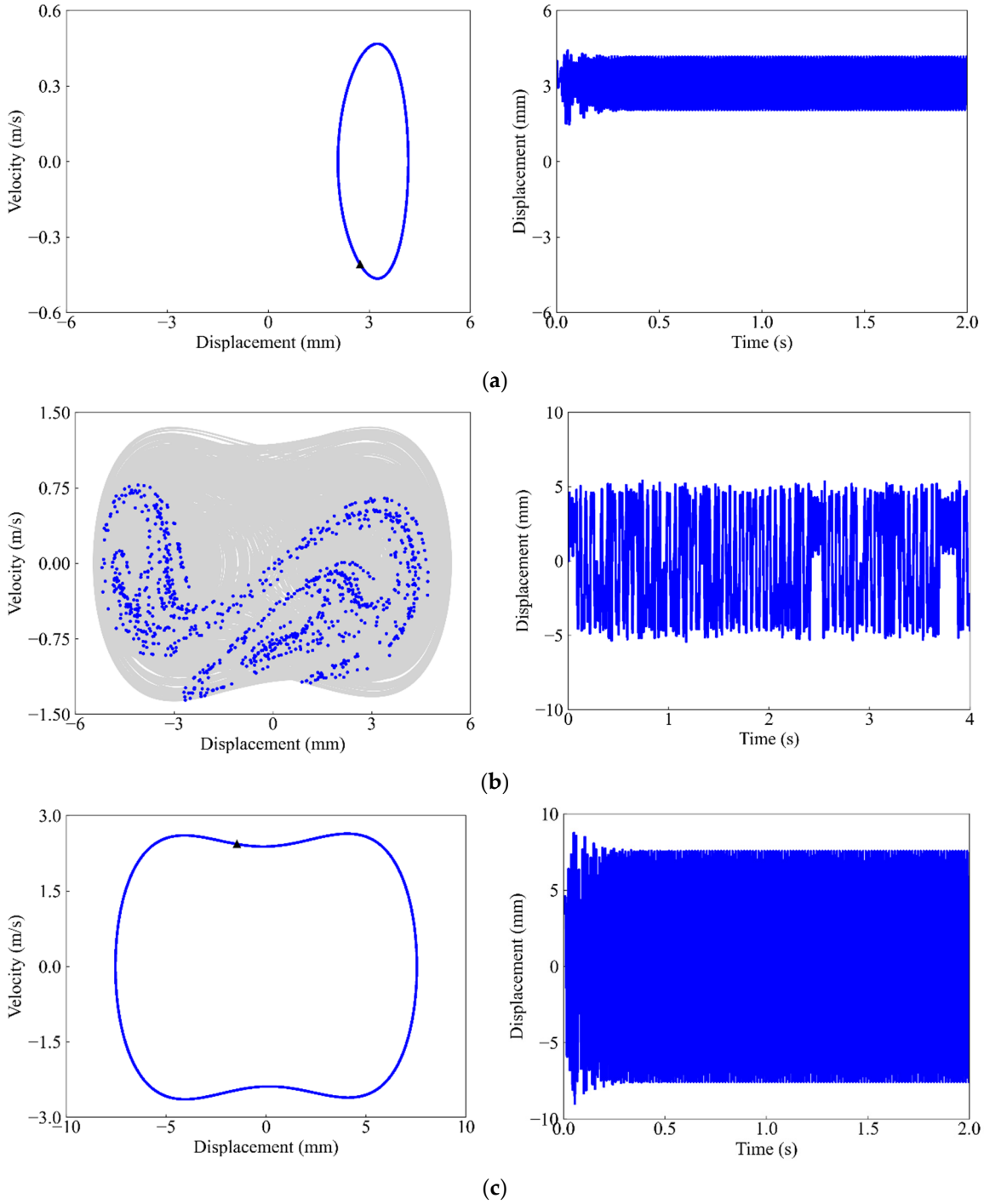

Figure 6. Reduced-order model analysis considering an excitation frequency of 70 Hz. Phase space and displacement time-history for different excitation amplitudes: (**a**) Intra-well response (0.15 mm); (**b**) chaotic response (0.4 mm); and (**c**) inter-well response (1.0 mm). The blue and gray solid lines represent the time-history, while the black and blue markers represent the Poincare's section.

Once again, an excitation frequency of 70 Hz is adopted and initially, consider a base excitation of 0.15 mm amplitude. Figure 7a presents the system response showing a periodic pattern with small intra-well oscillation, generating an rms voltage about 0.8 V. A chaotic-like response is obtained by increasing the base excitation amplitude for 0.4 mm, Figure 7b, an inter-well response where external energy is enough to visit both stable equilibrium points, and generating an rms voltage of 2.2 V. The Poincaré section of this response shows a strange attractor illustrated in Figure 7b. A new increase in the external

amplitude to 1 mm is in response to a periodic inter-well that generates an output voltage of 4.6 V. It should be pointed out that the different kinds of response are directly associated with the energy harvesting capacity, clearly establishing the connection between collected energy and dynamics.

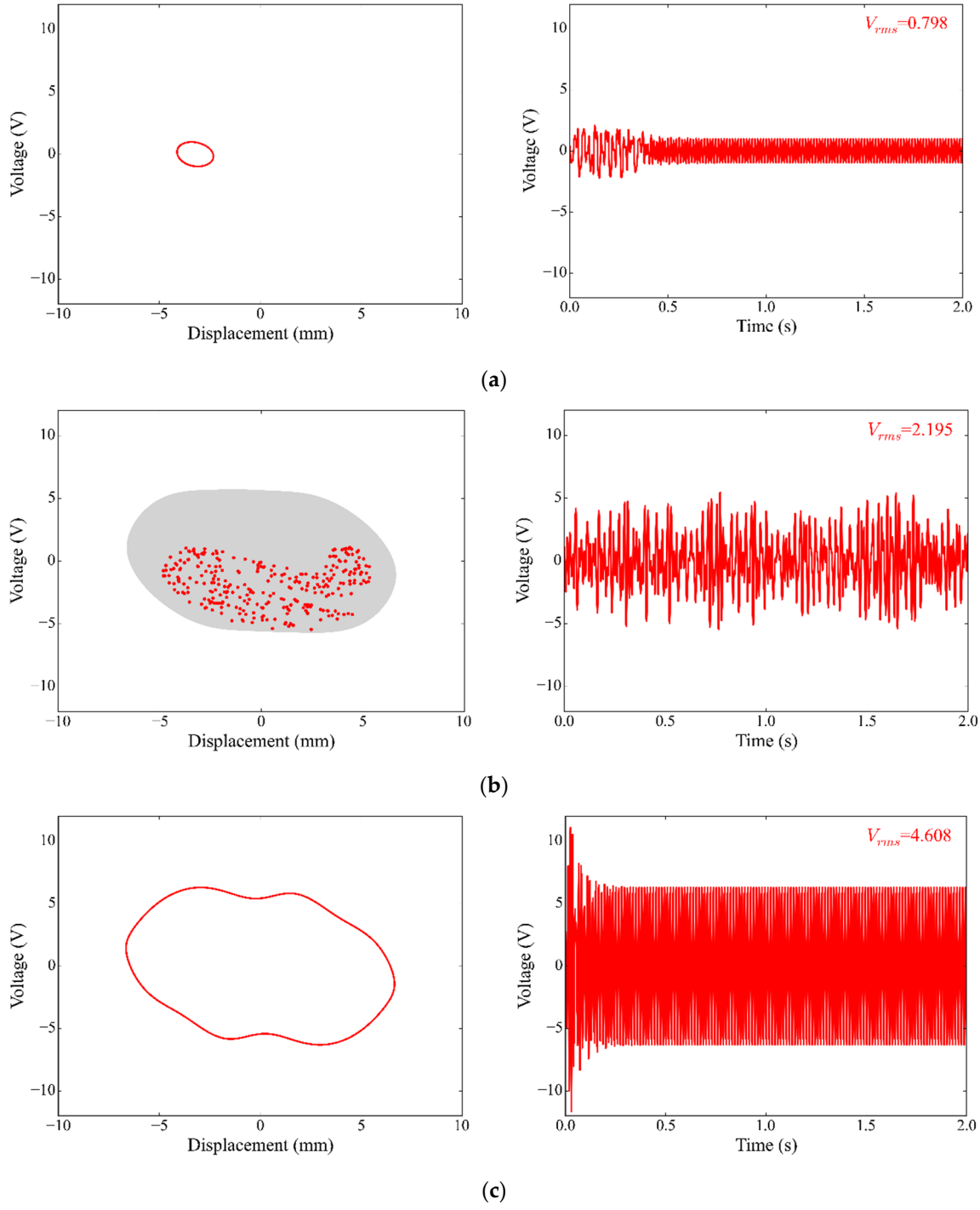

Figure 7. FE model analysis considering an excitation frequency of 70 Hz. Phase space and output voltage time-history for different excitation amplitudes: (**a**) Intra-well response (0.15 mm); (**b**) chaotic response (0.4 mm); and (**c**) inter-well response (1.0 mm). The red and gray solid lines represent the time-history response, while the red markers represent the Poincare's section.

Overall, the results demonstrate that the nonlinear FE model represents the general dynamical characteristics of the reduced-order model, qualitatively capturing the specific

behaviors of the energy harvesting system. This shows its effectiveness in analyzing complex system dynamics. The system richness is essentially related to nonlinearities, represented by the magnetic interactions. In this regard, the magnets create new dynamical possibilities that are exploited for energy harvesting purposes. Therefore, the linear energy harvester is represented by neglecting the magnetic interactions.

The linear energy harvesting presents better performance under resonant conditions and, since the beam is a continuous system, there are several possibilities to be exploited. On this basis, a harmonic analysis of the linear system is performed considering a frequency range of 0 to 1 kHz and an external amplitude of 0.2 mm. The equivalent linear system is obtained by neglecting the magnetic interactions, vanishing the magnetic forces. The amplitude response curve of the equivalent linear system is presented in Figure 8, showing that the first two bending natural frequencies are 85 and 535 Hz. Notably, the second bending mode exhibits a wider bandwidth, but a lower peak amplitude compared with the fundamental mode.

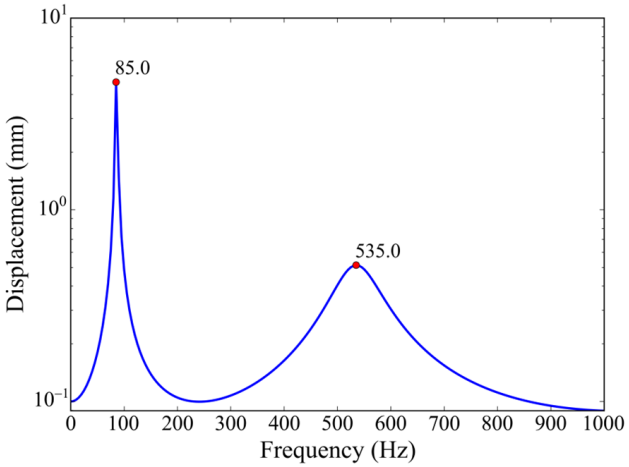

Figure 8. Frequency response curve for linear energy harvester.

Different operational conditions of the nonlinear energy harvester are now in focus using the linear frequency domain curve as a guide. Initially, consider an amplitude w_0 = 0.2 mm and three forcing frequencies below the first linear resonant peak: 35 Hz, 48 Hz and 50 Hz. Mechanical and electrical responses are represented by phase spaces and time-history output voltage being presented in Figure 9. The system presents periodic responses with high amplitude oscillations generating an rms voltage of 1.9 V for 35 Hz and 2.7 V for 48 Hz. By considering 50 Hz, a chaotic-like response is observed with an rms voltage of approximately 1.4 V. Note that there is a sudden change between 48 Hz and 50 Hz due to nonlinear effects.

The device performance is now investigated in a frequency region corresponding to the linear second vibration mode, around 535 Hz. It should be highlighted that a multimodal analysis is of concern, which is possibly due to the use of the FEM. The reduced-order model previously discussed was restricted to the first vibration mode and, therefore, does not capture this kind of response.

Consider an excitation amplitude of w_0 = 0.4 mm and two operating frequencies: 300 Hz, far away from resonant conditions; and 500 Hz, close to resonant condition. Figure 10 presents the system response for both cases, showing the phase space and the output voltage. At a frequency of 300 Hz, a typical periodic intra-well response is observed, with an rms voltage of 2.94 V. A comparison with Figure 7 can be made since the same excitation amplitude of 0.4 mm is employed. Note that the output voltage value is 34% bigger than the result obtained at 70 Hz (Figure 7b). In contrast, at 500 Hz, a periodic

response with an rms voltage of 16.85 V is reached, which is approximately 670% greater than the values of 70 Hz (Figure 7b). On this basis, it is noticeable that the high frequency response is better for energy harvesting purposes.

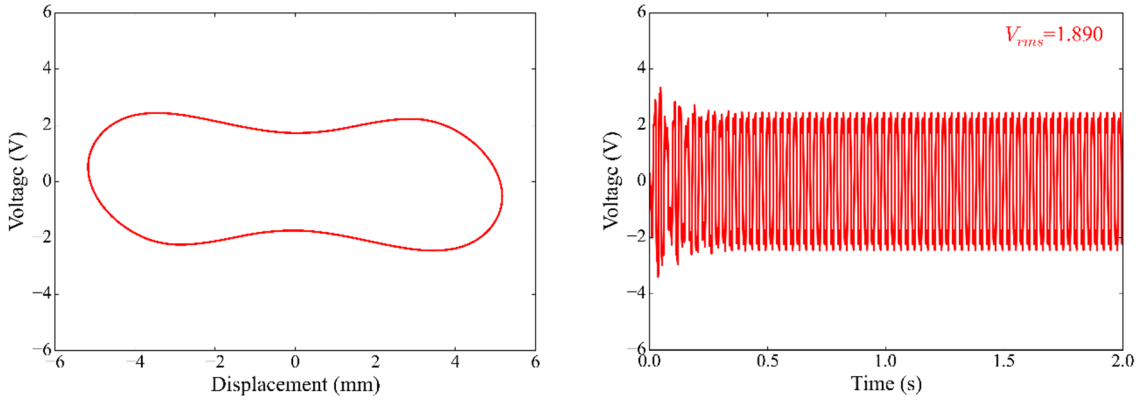

(**a**)

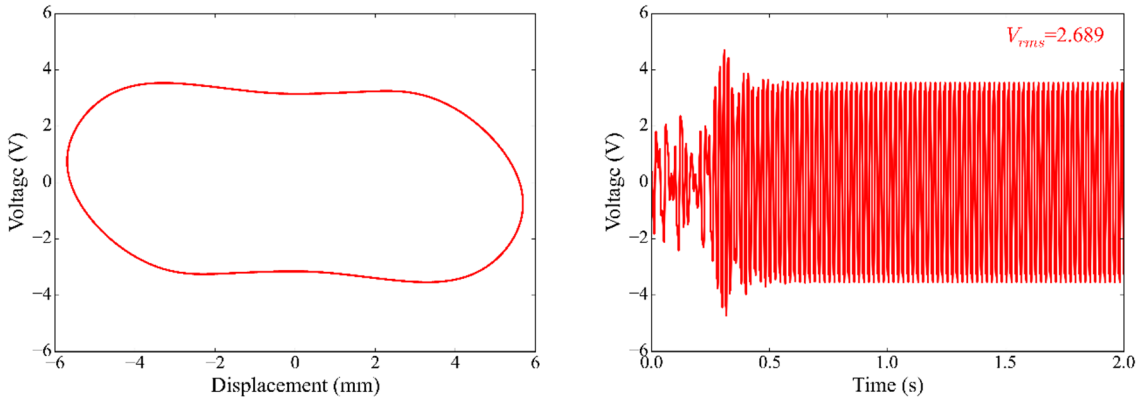

(**b**)

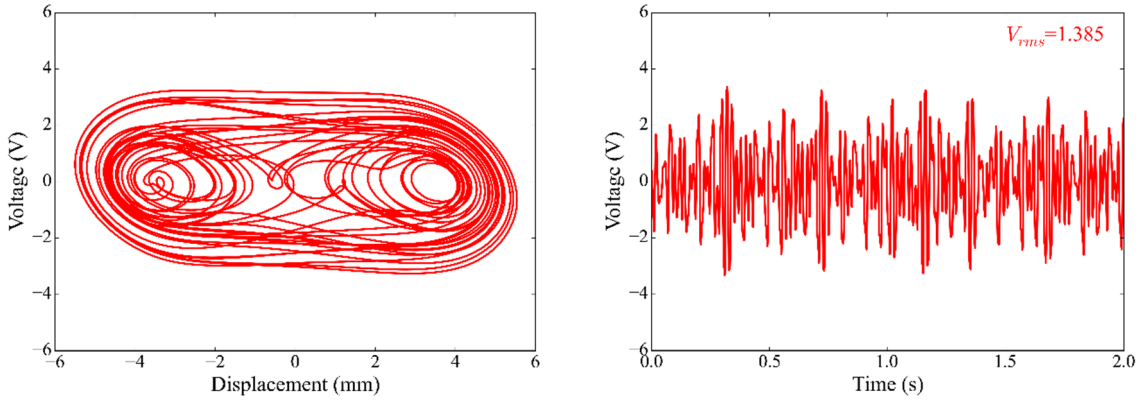

(**c**)

Figure 9. F Responses for frequencies smaller than the first resonant condition for base excitation of 0.2 mm. Phase space and output voltage time-history at steady-state condition for different excitation frequencies: (**a**) 35 Hz, (**b**) 48 Hz and (**c**) 50 Hz.

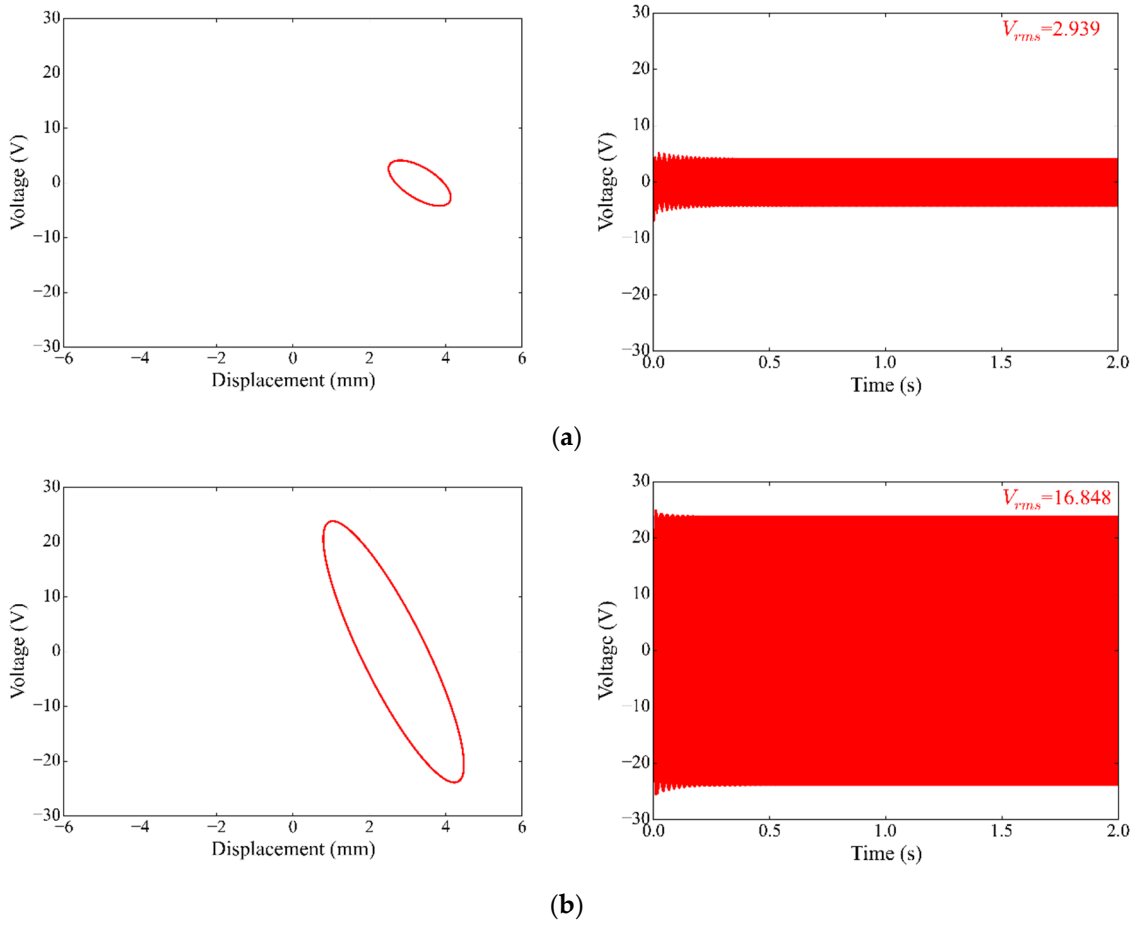

Figure 10. Response for frequencies bigger than the first resonant condition for base excitation of 0.4 mm. Phase space and output voltage time-history for different excitation frequencies: (**a**) 300 Hz and (**b**) 500 Hz.

These analyses show the importance of the nonlinear dynamical analysis. Additionally, it is shown that the energy harvesting can be performed in different vibration modes, highlighting the importance of a multimodal analysis.

4. Conclusions

This work deals with the analysis of a nonlinear vibration-based piezoelectric energy harvesting device using the finite element method. The energy harvesting device consists of a symmetrical beam having two piezoelectric materials bonded to an elastic substrate linear elastic beam. An electric circuit is connected to piezoelectric layers in a series configuration. Ambient mechanical vibrations are represented by base excitation, assumed to be harmonic. Nonlinearity due to magnetic interactions is represented by a cubic nonlinearity. The influence of multimode and nonlinear effects on system performance are investigated from numerical simulations, and energy harvesting capacity is analyzed by monitored harvested power.

A framework analysis is proposed combining the nonlinear finite element method with a reduced-order model that guides the nonlinear dynamical analysis. Simulations are carried out for different operational conditions represented by base excitation amplitudes and in a frequency range corresponding to first and second resonant conditions. The FE simulations are capable of capturing the rich dynamics characteristic of bistable systems presenting periodic and non-periodic responses with low and high energy oscillation amplitudes. Although, the first resonant condition is predominant for the system performance,

results show that, for high vibration amplitudes, the second resonant condition is also capable of generating enough energy to be used low-power-consuming devices. The FEM has demonstrated to be an interesting tool to design complex, multimodal and nonlinear energy harvesting devices in order to enhance the system performance.

This work emphasized that the design of energy harvesting devices is essentially related to nonlinear dynamics analysis and, therefore, the proposed framework is useful to guide the search for novel configurations. The combination of the finite element method with the reduced-order model is an interesting approach to deal with complex dynamical responses, treating multimodal systems.

Author Contributions: Conceptualization, V.J.C. and M.A.S.; methodology, V.J.C. and M.A.S.; software, V.J.C.; validation, V.J.C. and M.A.S.; formal analysis, V.J.C. and M.A.S.; investigation, V.J.C. and M.A.S.; resources, M.A.S.; data curation, V.J.C. and M.A.S.; writing—original draft preparation, V.J.C.; writing—review and editing, M.A.S.; visualization, V.J.C.; supervision, M.A.S.; project administration, M.A.S.; funding acquisition, M.A.S. All authors have read and agreed to the published version of the manuscript.

Funding: The authors would like to acknowledge the support of the Brazilian Research Agencies CNPq (Conselho Nacional de Desenvolvimento Científico e Tecnológico), CAPES (Coordenação de Aperfeiçoamento de Pessoal de Nível Superior), and FAPERJ (Fundação Carlos Chagas Filho de Amparo à Pesquisa do Estado do Rio de Janeiro) and through the INCT-EIE (National Institute of Science and Technology—Smart Structures in Engineering), and FAPEMIG (Fundação de Amparo à Pesquisa do Estado de Minas Gerais). The support of the AFOSR (Air Force Office of Scientific Research) (FA9550-23-4301-0527) is also acknowledged.

Institutional Review Board Statement: Not applicable.

Informed Consent Statement: Not applicable.

Data Availability Statement: The raw data supporting the conclusions of this article will be made available by the authors on request.

Conflicts of Interest: The authors declare no conflicts of interest.

References

1. Johnson, T.J.; Charnegie, D.; Clark, W.W.; Buric, M.; Kusic, G. *Energy Harvesting from Mechanical Vibrations using Piezoelectric Cantilever Beams*; The International Society for Optical Engineering: San Diego, CA, USA, 2006.
2. Sodano, H.A.; Park, G.; Inman, D.J. Estimation of Electric Charge Output for Piezoelectric Energy Harvesting. *Strain J.* **2004**, *40*, 49–58. [CrossRef]
3. Ng, T.-H.; Liao, W.-H. *Feasibility Study of a Self-Powered Piezoelectric Sensor*; SPIE-The International Society for Optical Engineering: San Diego, CA, USA, 2004; pp. 377–388.
4. Ng, T.-H.; Liao, W.-H. Sensitivity Analysis and Energy Harvesting for a Self-Powered Piezoelectric Sensor. *J. Intell. Mater. Syst. Struct.* **2005**, *16*, 758–797. [CrossRef]
5. Erturk, A.; Inman, D.J. An Experimentally Validated Bimorph Cantilever Model for Piezoelectric Energy Harvesting from Base Excitations. *Smart Mater. Struct.* **2009**, *18*, 025009. [CrossRef]
6. Erturk, A.; Renno, J.M.; Inman, D.J. Modeling of Piezoelectric Energy Harvesting from an L-shaped Beam-mass Structure with an Application to UAVs. *J. Intell. Mater. Syst. Struct.* **2009**, *20*, 529–554. [CrossRef]
7. Erturk, A.; Inman, D.J. On Mechanical Modeling of Cantilevered Piezoelectric Vibration Energy Harvesters. *J. Intell. Mater. Syst. Struct.* **2008**, *19*, 1311–1325. [CrossRef]
8. Erturk, A.; Inman, D.J. A Distributed Parameter Electromechanical Model for Cantilevered Piezoelectric Energy Harvesters. *J. Vib. Acoust.* **2008**, *130*, 041002. [CrossRef]
9. Erturk, A.; Inman, D.J. Issues in Mathematical Modeling of Piezoelectric Energy Harvesters. *Smart Mater. Struct.* **2008**, *17*, 065016. [CrossRef]
10. Tang, L.; Yang, Y.; Soh, C.K. Toward Broadband Vibration-Based Energy Harvesting. *J. Intell. Mater. Syst. Struct.* **2010**, *21*, 1867–1897. [CrossRef]

11. Zhu, D.; Tudor, M.J.; Beeby, S.P. Strategies for Increasing the Operating Frequency Range of Vibration Energy Harvesters: A Review. *Meas. Sci. Technol.* **2009**, *21*, 022001. [CrossRef]
12. Shahruz, S.M. Design of mechanical band-pass filters for energy scavenging. *J. Sound Vib.* **2006**, *292*, 987–998. [CrossRef]
13. Lin, H.C.; Wu, P.H.; Lien, I.C.; Shu, Y.C. Analysis of an array of piezoelectric energy harvesters connected in series. *Smart Mater. Struct.* **2013**, *22*, 094026. [CrossRef]
14. Kim, I.H.; Jung, H.J.; Lee, B.M.; Jang, S.J. Broadband Energy-harvesting Using a Two Degree-of-freedom Vibrating Body. *Appl. Phys. Lett.* **2011**, *98*, 214102. [CrossRef]
15. Ou, Q.; Chen, X.; Gutschmidt, S.; Wood, A.; Leigh, N. A Two-mass Cantilever Beam Model for Vibration Energy Harvesting Applications. In Proceedings of the 2010 IEEE International Conference on Automation Science and Engineering, Toronto, ON, Canada, 21–24 August 2010; pp. 301–306.
16. Tadesse, Y.; Zhang, S.; Priya, S. Multimodal Energy Harvesting System: Piezoelectric and Electromagnetic. *Intell. Mater. Syst. Struct.* **2009**, *20*, 625–632. [CrossRef]
17. Tang, L.; Yang, Y. A multiple-degree-of-freedom piezoelectric energy harvesting model. *Intell. Mater. Syst. Struct.* **2012**, *23*, 1631–1647. [CrossRef]
18. Wu, H.; Tang, L.; Yang, Y.; Soh, C.K. A Novel Two-degrees-of-freedom Piezoelectric Energy Harvester. *Intell. Mater. Syst. Struct.* **2013**, *24*, 357–368. [CrossRef]
19. Caetano, V.J.; Savi, M.A. Multimodal pizza-shaped piezoelectric vibration-based energy harvesters. *J. Intell. Mater. Syst. Struct.* **2021**, *32*, 2505–2528. [CrossRef]
20. Caetano, V.J.; Savi, M.A. Star-shaped Piezoelectric Mechanical Energy Harvesters for Multidirectional Sources. *Int. J. Mech. Sci.* **2021**, *215*, 106962. [CrossRef]
21. Costa, L.G.; Savi, M.A. Nonlinear dynamics of a compact and multistable mechanical energy harvester. *Int. J. Mech. Sci.* **2024**, *262*, 108731. [CrossRef]
22. Costa, L.G.; Monteiro, L.L.S.; Savi, M.A. Multistability investigation for improved performance in a compact nonlinear energy harvester. *J. Braz. Soc. Mech. Sci. Eng.* **2024**, *46*, 4. [CrossRef]
23. Costa, L.G.; Monteiro, L.L.D.S.; Pacheco, P.M.C.L.; Savi, M.A. A parametric analysis of the nonlinear dynamics of bistable vibration-based piezoelectric energy harvesters. *J. Intell. Mater. Syst. Struct.* **2021**, *32*, 699–723. [CrossRef]
24. Zhang, L.; Lan, C.; Lu, F.; Lu, Y. Theoretical Analysis of the Power Performance of a Monostable Galloping-Based Piezoelectric Energy Harvester. *Int. J. Energy Res.* **2024**, *2024*, 1386237. [CrossRef]
25. Upadrashta, D.; Yang, Y. Nonlinear piezomagnetoelastic harvester array for broadband energy harvesting. *J. Appl. Phys.* **2016**, *120*, 054504. [CrossRef]
26. Yan, Z.; Sun, W.; Hajj, M.R.; Zhang, W.; Tan, T. Ultra-broadband piezoelectric energy harvesting via bistable multi-hardening and multi-softening. *Nonlinear Dyn.* **2020**, *100*, 1057–1077. [CrossRef]
27. Kim, J.; Dorin, P.; Wang, K.W. Vibration energy harvesting enhancement exploiting magnetically coupled bistable and linear harvesters. *Smart Mater. Struct.* **2020**, *29*, 065006. [CrossRef]
28. Leng, Y.; Tan, D.; Liu, J.; Zhang, Y.; Fan, S. Magnetic force analysis and performance of a tri-stable piezoelectric energy harvester under random excitation. *J. Sound Vib.* **2017**, *406*, 146–160. [CrossRef]
29. Cao, Y.Y.; Yang, J.H.; Yang, D.B. Dynamically synergistic transition mechanism and modified nonlinear magnetic force modeling for multistable rotation energy harvester. *Mech. Syst. Signal Process.* **2023**, *189*, 110085. [CrossRef]
30. Fu, H.; Jiang, J.; Hu, S.; Rao, J.; Theodossiades, S. A multi-stable ultra-low frequency energy harvester using a nonlinear pendulum and piezoelectric transduction for self-powered sensing. *Mech. Syst. Signal Process.* **2023**, *189*, 110034. [CrossRef]
31. Wang, C.; Zhang, Q.; Wang, W. Wideband quin-stable energy harvesting via combined nonlinearity. *AIP Adv.* **2017**, *7*, 4. [CrossRef]
32. Tang, L.; Yang, Y.; Soh, C.K. Improving functionality of vibration energy harvesters using magnets. *J. Intell. Mater. Syst. Struct.* **2012**, *23*, 1433–1449. [CrossRef]
33. Cottone, F.; Gammaitoni, L.; Vocca, H.; Ferrari, V. Piezoelectric Buckled Beams for Random Vibration Energy Harvesting. *Smart Mater. Struct.* **2012**, *21*, 035021. [CrossRef]
34. Erturk, A.; Inman, D.J. Broadband Piezoelectric Power Generation on High-energy Orbits of the Bistable Duffing Oscillator with Electromechanical Coupling. *J. Sound Vib.* **2011**, *330*, 2339–2353. [CrossRef]
35. Zhou, S.; Cao, J.; Inman, D.J.; Lin, J.; Liu, S.; Wang, Z. Broadband tristable energy harvester: Modeling and experiment verification. *Appl. Energy* **2014**, *133*, 33–39. [CrossRef]
36. Erturk, A.; Hoffmann, J.; Inman, D.J. A piezomagnetoelastic Structure for Broadband Vibration Energy Harvesting. *Appl. Phys. Lett.* **2009**, *94*, 254102. [CrossRef]
37. Stanton, S.C.; Mcgehee, C.C.; Mann, B.P. Nonlinear Dynamics for Broadband Energy Harvesting: Investigation of a Bistable Piezoelectric Inertial Generator. *Phys. D* **2010**, *239*, 640–653. [CrossRef]
38. Ferrari, M.; Baù, M.; Guizzetti, M.; Ferrari, V. A Single-magnet Nonlinear Piezoelectric Converter for Enhanced Energy Harvesting from Random Vibrations. *Sens. Actuators: A. Phys.* **2011**, *172*, 287–292. [CrossRef]

39. DePaula, A.S.; Inman, D.J.; Savi, M.A. Energy Harvesting in a Nonlinear Piezomagnetoelastic Beam Subjected to Random Excitation. *Mech. Syst. Signal Process.* **2015**, *54*, 405–416. [CrossRef]
40. Reis, E.V.; Savi, M.A. Spatiotemporal nonlinear dynamics and chaos in a mechanical Duffing-type system. *Chaos Solitons Fractals* **2024**, *185*, 115177. [CrossRef]
41. Zhu, M.; Worthington, E.; Njuguna, J. Analyses of Power Output of Piezoelectric Energy-Harvesting Devices Directly Connected to a Load Resistor Using a Coupled Piezoelectric-Circuit Finite Element Method. *IEEE Trans. Ultrason. Ferroelectr. Freq. Control* **2009**, *56*, 1309–1318. [CrossRef]
42. Abdelkefi, A.; Barsallo, N.; Tang, L.; Yang, Y.; Hajj, M.R. Modeling, Validation, and Performance of Low-Frequency Piezoelectric Energy Harvesters. *J. Intell. Mater. Syst. Struct.* **2014**, *25*, 1429–1444. [CrossRef]
43. Upadrashta, D.; Yang, Y. Finite Element Modeling of Nonlinear Piezoelectric Energy Harvesters with Magnetic Interaction. *Smart Mater. Struct.* **2015**, *24*, 045042. [CrossRef]
44. Li, J.; Zhang, X.; Jiang, W.; Bi, Q.; Chen, L. A novel cut-out piezoelectric beam with limiters for broadband energy harvesting. *Int. J. Non-Linear Mech.* **2024**, *167*, 104919. [CrossRef]
45. Kim, P.; Seok, J. Dynamic and Energetic Characteristics of a Tri-Stable Magnetopiezoelastic Energy Harvester. *Mech. Mach. Theory* **2015**, *94*, 41–63. [CrossRef]
46. Kim, P.; Seok, J. A multi-stable energy harvester: Dynamic modeling and bifurcation analysis. *J. Sound Vib.* **2014**, *333*, 5525–5547. [CrossRef]
47. ANSYS Academic Research, Release 17.2. In Help System, Theory Reference, 15. Analysis Procedures: Transient Analysis. Available online: https://www.mm.bme.hu/~gyebro/files/ans_help_v182/ans_thry/thy_anproc2.html (accessed on 1 September 2019).